



## HEESCH NUMBERS OF UNMARKED POLYFORMS

CRAIG S. KAPLAN

**ABSTRACT.** A shape's Heesch number is the number of layers of copies of the shape that can be placed around it without gaps or overlaps. Experimentation and exhaustive searching have turned up examples of shapes with finite Heesch numbers up to six, but nothing higher. The computational problem of classifying simple families of shapes by Heesch number can provide more experimental data to fuel our understanding of this topic. I present a technique for computing Heesch numbers of nontiling polyforms using a SAT solver, and the results of exhaustive computation of Heesch numbers up to 19-ominoes, 17-hexes, and 24-diamonds.

### 1. INTRODUCTION

Tiling theory is the branch of mathematics concerned with the properties of shapes that can cover the plane with no gaps or overlaps. It is a topic rich with deep results and open problems. Of course, tiling theory must occasionally venture into the study of shapes that *do not* tile the plane so that we might understand those that do more completely.

If a shape tiles the plane, then it must be possible to surround the shape with congruent copies of itself, leaving no part of its boundary exposed. A circle clearly cannot tile the plane, because neighbouring circles can cover at most a finite number of points on its boundary. A regular pentagon also cannot be surrounded by copies of itself: its vertices will always remain exposed.

However, the converse is not true: there exist shapes that can be fully surrounded by copies of themselves, but for which no such surround can be extended to a tiling. For example, there are 108 heptominoes (shapes formed by gluing together seven squares), of which four, shown in Figure 1, are known not to tile the plane. One of them contains an internal hole and can be discarded immediately. As it happens, the other three can all be surrounded. In the middle two cases, the shape and its surrounding copies are simply connected. On the right, the surrounding tiles leave behind an internal hole, and no alternative surround can eliminate that hole.

---

Received by the editors June 23, 2021, and in revised form July 29, 2021.

This work is licensed under a Creative Commons “Attribution-NoDerivatives 4.0 International” license.



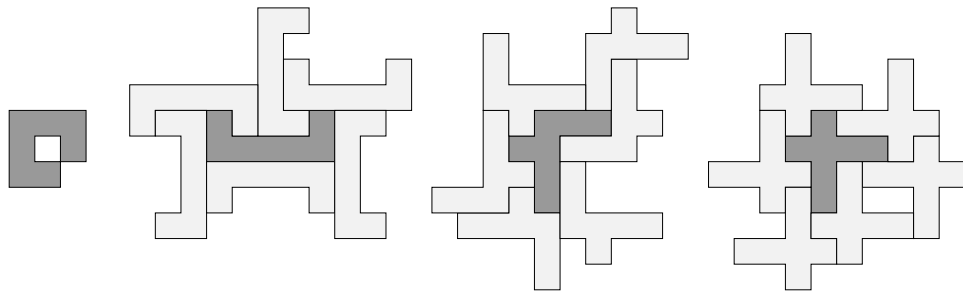


FIGURE 1. The four nontiling heptominoes. The shape on the left has a hole and cannot be surrounded. The other three can be fully surrounded by copies, but in the rightmost shape the copies will necessarily enclose a hole.

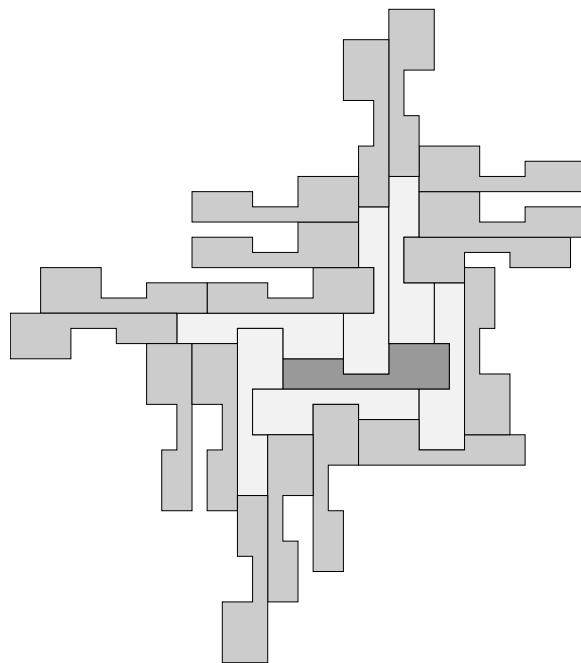


FIGURE 2. A 23-omino that can be surrounded by two layers of copies of itself, but not more.

There is no a priori reason why a given nontiling shape might not be surroundable by two, three, or more layers of copies of itself. The illustrations in Figure 1 provide lower bounds for the number of layers for these shapes; that they also represent upper bounds must be proven by enumerating all possible surrounds, and showing that none of them may be further

surrounded. Other shapes might permit more layers. For example, the 23-omino shown in Figure 2, due to Fontaine [4], can be surrounded by two layers but not more. How far can this process be extended?

A shape's *Heesch number* is the number of times it can be surrounded with complete layers of congruent copies of itself (I will offer a precise definition in the next section). If the shape tiles the plane, its Heesch number is defined to be infinity. *Heesch's problem* asks which positive integers are Heesch numbers; that is, for which  $n > 0$  does there exist a shape with Heesch number  $n$ ?

Very little is known about the solution to Heesch's problem. Writing in 1987, Grünbaum and Shephard were not aware of any examples with finite Heesch number greater than 1 [6, section 3.8]. After that, a few isolated examples were found with Heesch numbers up to 4 [9]. Mann and Thomas performed a systematic computer search of marked polyforms (polyominoes, polyhexes, and polyiamonds, with edges decorated by geometric matching conditions), yielding new examples and pushing the record to 5 [10]. In 2021 Bašić finally broke this record, demonstrating a figure with Heesch number 6 [2].

The study of Heesch numbers can shed light on some of the deepest problems in tiling theory. In particular, the *tiling problem* asks, for a given set of shapes, whether they admit at least one tiling of the plane. The tiling problem is known to be undecidable for general sets of shapes [3], but its status is open for a set consisting of a single shape  $S$ . If there were an upper bound  $N$  on finite Heesch numbers, then the tiling problem would be decidable, at least when there are only finitely many ways that two copies of  $S$  may be adjacent [5]. The algorithm would involve trying the finitely many ways of surrounding  $S$  with  $N + 1$  layers of copies of itself. If you succeed, then you have exceeded the maximum finite Heesch number and  $S$  must tile the plane. If you fail, then  $S$  evidently does not tile. To that end, more experimental data revealing which Heesch numbers are possible, even for limited classes of shapes, could be useful in understanding whether such an upper bound might exist.

In this article, I report on a complete enumeration of Heesch numbers of unmarked polyforms, up to 19-ominoes, 17-hexes, and 24-iamonds. This enumeration comprises approximately 4.16 billion nontilers, extracted from enumerations of all free polyforms of those sizes. Respecting a slight difference of opinion among researchers, I compute two variations of Heesch numbers: one where tiles may form holes in the outermost layer, and one where a shape and all its surrounding layers must be simply connected. This enumeration does not shatter the existing records for Heesch numbers, but it does provide a store of new examples of shapes with nontrivial Heesch numbers. Some, like a 9-omino with Heesch number 2 (Figure 7) and a 7-hex with Heesch number 3 (Figure 8), are interesting because of the complex behaviour exhibited by relatively simple shapes. The enumeration also uncovered seven new examples with Heesch number 4.

Apart from the tabulation and specific examples, the other main contribution of this work lies in the use of a SAT solver to compute Heesch numbers. Because polyominoes, polyhexes, and polyiamonds are subsets of ambient regular tilings of the plane, it is possible to reduce the geometric problem of surroundability to the logical problem of satisfiability of Boolean formulas. A SAT solver can optimize its search of the exponential space of possible solutions, avoiding the risk of “backtracking hell”. This formulation leads to a very reliable algorithm, whose performance degrades only on the rare shapes that actually have high Heesch numbers.

## 2. MATHEMATICAL BACKGROUND

Although Heesch’s problem grew out of tiling theory, most of the language, techniques, and results of tiling theory are not needed within the scope of this article and will be omitted. Readers interested in the topic should consult Grünbaum and Shephard’s book [6], which remains the standard reference. In this section, I will formalize the definition of a shape’s Heesch number and review marked and unmarked polyforms.

**2.1. Heesch numbers.** Let  $C$  and  $S$  be simple shapes in the plane, i.e., topological discs. We say that  $C$  can be *surrounded by*  $S$  if there exists a set of shapes  $\{S_1, \dots, S_n\}$  with the following properties:

- (1) Each  $S_i$  is congruent to  $S$  via a rigid motion in the plane;
- (2) The shapes in the set  $\{C, S_1, \dots, S_n\}$  have pairwise disjoint interiors;
- (3) The boundary of each  $S_i$  shares at least one point with the boundary of  $C$ .
- (4) The boundary of  $C$  lies entirely within the interior of the union of  $C$  and all the  $S_i$ .

The second condition forces the shapes not to overlap, except on their boundaries. The third condition forces every  $S_i$  to be useful in covering the boundary of  $C$ . The fourth condition ensures that  $C$  is completely surrounded.

If, furthermore, the union of  $C$  and the  $S_i$  is simply connected, we say that  $C$  can be surrounded by  $S$  *without holes*. In tiling theory, a finite union of nonoverlapping shapes whose union is a topological disc is also known as a *patch*, a term I will use here. On the other hand, I will use the more general term *packing* when shapes are known to be nonoverlapping but when their union may or may not contain holes.

We formalize the notion of layers by defining the *coronas* of  $S$ . We define the 0-corona of  $S$  to be the singleton set  $\{S\}$ . Setting  $C = S$  above, if  $S$  can be surrounded by itself then the tiles that make up that surround are one possible 1-corona of  $S$ . In general, if we have a nested sequence of  $k$ -coronas for  $k = 0, \dots, n - 1$ , all without holes, and the patch created from the union of all of these coronas can itself be surrounded by  $S$ , then the copies of  $S$  making up the surround constitute an  $n$ -corona.

The *Heesch number* of a shape  $S$  is the largest  $n$  for which  $S$  has an  $n$ -corona. If  $S$  tiles the plane, then by definition it is possible to build an  $n$ -corona for every positive integer  $n$ , and we define its Heesch number to be infinity. If we wish to be concise, we will simply say that  $S$  has  $H = n$ .

The definitions above require that for a shape to have Heesch number  $n$ , each  $k$ -corona for  $k = 1, \dots, n - 1$  surround its predecessor without holes. But it leaves the status of the outermost corona ambiguous. Most researchers require that a shape's  $n$ -corona be hole-free in order to regard the shape as having  $H = n$ , but some permit the  $n$ -corona to have holes. In this article, I will remain neutral on this point, and report separate results with and without holes in the outer corona. To that end, I will say that a shape has  $H_c = n_1$  and  $H_h = n_2$  to distinguish its Heesch numbers when holes are forbidden or permitted in the outer corona, respectively. In any case, we must always have either  $H_c = H_h$  or  $H_c = H_h - 1$ , so this difference of opinion cannot affect results too dramatically. Note that permitting a hole in the outermost corona raises the alarming possibility that the hole could be filled with additional shapes, forcing us to consider the validity of a subsequent corona made from multiple disjoint pieces!

**2.2. Polyforms.** A *polyform* is a shape constructed by gluing together multiple copies of some simple polygonal building block along their edges. Usually, we require that the assembly be *edge-to-edge*: no vertex of one copy of the building block may lie in the middle of the edge of another copy. The most famous polyforms are the *polyominoes*, constructed from glued-together squares. We speak more specifically of *n-ominoes* as unions of  $n$  squares, so that, for example, the 4-ominoes (or tetrominoes) are the familiar Tetris pieces. In this article, I will also consider *polyhexes* and *polyiamonds*, formed from unions of regular hexagons and unions of equilateral triangles, respectively, and refer more precisely to *n-hexes* and *n-iamonds* as needed.

Simple polyforms are an attractive domain in which to compute Heesch numbers. They can be explored exhaustively by enumerating the finite number of distinct  $n$ -forms for each successive  $n$ . The edge-to-edge constraint often reduces a continuous geometric problem to a combinatorial one, and in the technique presented here, even the combinatorial structure will be distilled into a problem in Boolean satisfiability. Still, polyforms can expose many of the core behaviours of shapes more generally. Conceivably one could establish an upper bound on Heesch numbers of, say, polyominoes, while leaving Heesch's problem open more generally; but in the meantime, these calculations can yield a trove of interesting data.

In a *marked* polyform, the edges of a polyform are assigned symbolic labels, and a binary relation over labels determines which pairs of edges may be placed side-by-side in neighbouring copies of the polyform. A simple system of labels involves marking some edges with a “bump”, some with a corresponding “nick”, and leaving all others flat. Flat edges can only meet other flat edges, and bumps must be adjacent to nicks. Mann and

Thomas computed Heesch numbers of simple polyforms with markings of this form [10]. They began with a small family of low-order polyominoes, polyhexes, and polyiamonds, enumerated all possible assignments of bumps and nicks to their edges, and computed the Heesch numbers of the resulting shapes using a recursive search with backtracking. Their search yielded a number of examples with Heesch numbers up to 5. However, the majority of their efforts produced inconclusive results: they either failed to produce a finite Heesch number in the time allotted to each shape or terminated the computation at five coronas. The main reason for this deficiency is that they did not have an effective procedure for first computing whether a marked polyform tiles the plane. Most of their inconclusive results are likely to be shapes with Heesch numbers that are infinite, rather than high-but-finite.

To my knowledge, no previous work has sought to compute Heesch numbers of *unmarked* polyforms. Myers tabulated information about polyominoes, polyhexes, and polyiamonds that tile the plane [11]. He determined whether polyforms tiled in progressively more intricate ways, measuring the *isohedral number* of tilers (roughly speaking, the number of copies of the tile that must be glued together to produce a patch that tiles in a relatively simple way). Each of his tables includes a single column labelled “nontilers”. This article sorts that column into multiple bins organized by Heesch number, effectively tabulating the progressively more intricate ways in which polyforms *do not* tile. Myers’s software is remarkably efficient, requiring on average a fraction of a millisecond on modern hardware to classify a given polyform. I use his software to produce initial lists of nontilers for Heesch number computation, thereby avoiding the needless construction of coronas for shapes that have infinitely many of them.

### 3. COMPUTING HEESCH NUMBERS WITH A SAT SOLVER

In this section, I show how to reduce the problem of computing a polyform’s Heesch number to evaluating the satisfiability of a sequence of Boolean formulas. At a high level, each formula encodes whether a given polyform has a Heesch number of at least  $n$  (with slight variations depending on whether to allow holes). I check the satisfiability of these formulas for increasing values of  $n$  until I find one that is unsatisfiable, indicating the nonexistence of a corona of a given level.

Every formula will be expressed in *conjunctive normal form* (CNF) as a conjunction of clauses, each of which is a disjunction of variables or their negations. That is, each clause ORs together any number of Boolean variables or their negations, and the entire formula is an AND of clauses. I use the standard operators  $\vee$  for OR,  $\wedge$  for AND, and  $\neg$  for NOT. I will also allow clauses to be written using an implication operator with a single variable on the left, converting  $x \rightarrow Q$  to  $\neg x \vee Q$  as needed.

To simplify the exposition, I will limit the development here exclusively to polyominoes. In the next section, I will describe the modifications that are necessary to support polyhexes and polyiamonds.

**3.1. Developing the base formula.** Because shapes always meet edge-to-edge, we can assume that they occupy cells in a conceptually infinite grid of squares, indexed by  $(x, y)$  pairs of integer coordinates. For a given cell  $p = (x, y)$ , define  $N_8(p)$ , the 8-neighbourhood of  $p$ , to be the set of cells horizontally, vertically, or diagonally adjacent to  $p$ . Now let  $S$  be an  $m$ -omino whose Heesch number we wish to compute. We describe  $S$  as a set of cells  $\{(x_1, y_1), \dots, (x_m, y_m)\}$ , translated so that  $(0, 0) \in S$ . We will also make use of the *halo* of  $S$ , written  $\text{HALO}(S)$ , the set of grid cells  $p$  for which  $p \notin S$  but  $N_8(p) \cap S \neq \emptyset$ . That is,  $\text{HALO}(S)$  consists of a ring of cells around the boundary of  $S$ .

Ignoring symmetry, a polyomino has eight distinct rotated and reflected orientations, which can be represented by  $2 \times 2$  matrices with entries in  $\{-1, 0, 1\}$ . We must also track translations of polyominoes by integer vectors  $(\Delta x, \Delta y)$ . Any possible transformed copy of  $S$  can therefore be identified with six (usually small) integers that define an affine transformation  $T$ . Two transformed shapes  $T_1(S)$  and  $T_2(S)$  are *adjacent* if they occupy neighbouring cells but do not overlap; that is,  $T_1(S) \cap T_2(S) = \emptyset$ , but  $T_1(S) \cap \text{HALO}(T_2(S)) \neq \emptyset$ . For a fixed  $S$ , I will also refer to  $T_1$  and  $T_2$  as adjacent in this context.

We are particularly interested in finite sets of transformations  $\mathcal{T}_k$ , containing every possible  $T$  for which  $T(S)$  might be part of a  $k$ -corona of  $S$ . We can define these sets recursively by setting  $\mathcal{T}_0$  to be a singleton set containing the identity transformation, and each subsequent  $\mathcal{T}_k$  to be every transformation  $T$  adjacent to some  $T' \in \mathcal{T}_{k-1}$ . Every  $k$ -corona of  $S$ , if one exists, must consist of copies of  $S$  transformed by a subset of  $\mathcal{T}_k$ .

We are now ready to define two classes of Boolean variables: cell variables and shape variables. These will encode whether a given cell or a given transformation is actually used as part of a set of coronas. For every  $p = (x, y)$  in the grid, the *cell variable*  $c_p$  is true if and only if  $p$  is covered by some transformed copy of  $S$ . For every affine transformation  $T$  and every integer  $k \geq 0$ , the *shape variable*  $s_{T,k}$  is true if and only if the transformed shape  $T(S)$  is used as part of the  $k$ -corona in a packing of copies of  $S$ .

Conceptually, the clauses in a CNF formula are a tool for coupling together the behaviours of individual variables. For example, if we know that  $T_1(S) \cap T_2(S) \neq \emptyset$ , then these transformed shapes can never be used together in a patch. We can force them to be mutually exclusive with clauses of the form  $\neg s_{T_1,i} \vee \neg s_{T_2,j}$  for all coronas  $i$  and  $j$ . These clauses ensure that at least one of  $T_1(S)$  and  $T_2(S)$  is left out of any satisfying assignments. In the formulation presented here, cell variables act as mediators, allowing shape variables to exchange information with each other without having to refer to each other directly. For example, a clause of the form  $s_{T,k} \rightarrow c_j$

(or equivalently,  $\neg s_{T,k} \vee c_j$ ) allows a transformed shape to demand that a particular cell—say, one of its halo cells—be occupied. With a second clause of the form  $c_j \rightarrow s_{T_1,i_1} \vee s_{T_2,i_2} \vee \dots \vee s_{T_n,i_n}$ , that cell can then offer a menu of possible occupants. Clauses like these are the key to reducing the geometric problem of Heesch number computation to Boolean logic.

Given an integer  $n > 0$ , we can, at last, write down a Boolean formula  $F_n$  whose satisfiability implies that  $S$  has an  $n$ -corona.  $F_n$  is the conjunction of a large number of clauses, belonging to seven distinct classes. The clauses are listed in full in Figure 3, along with intuitive explanations of their meanings. Informally, we see that the 0-corona is activated by fiat, which in turn demands that its halo cells all be occupied by adjacent shapes. Additional clauses force those adjacent shapes to belong to the 1-corona and to be pairwise disjoint. A similar process plays out in each subsequent corona before the last one: shapes in the corona tag their halo cells, thereby recruiting new neighbours to surround them. The shapes in the outermost corona are left partially exposed to empty space.

The formula  $F_n$  can be given to a SAT solver, a program that consumes a Boolean formula and determines whether any assignment of true or false to its variables makes the entire formula true. If the solver reports that  $F_n$  is satisfiable, then the coronas of  $S$  can be read directly from the true variables  $s_{T,k}$  in the satisfying assignment. I iteratively construct and check  $F_n$  for each  $n \geq 1$  in turn; an unsatisfiable  $F_n$  implies that  $S$  has Heesch number  $n - 1$ . Unfortunately,  $F_n$  does not contain a strict superset of the clauses of  $F_{n-1}$  and must be constructed starting from scratch.

**3.2. Suppressing holes.** If  $F_n$  is satisfiable, then the subset of shapes out to the  $(n - 1)$ -corona will be a simply connected patch: every shape’s halo must be filled, and so no pockets of empty space can be left behind. However, there is nothing to prohibit holes from forming between shapes in the  $n$ -corona. Thus the algorithm above can compute only whether  $S$  has  $H_h = n$ . If we wish to compute the hole-free Heesch number  $H_c$ , then we must suppress all holes in the outermost corona.

Most such holes that might arise are relatively simple and can be suppressed easily. These are holes that are completely enclosed by a pair of adjacent shapes in the  $n$ -corona (Figure 4, centre). I precompute all pairs of transforms  $T_1, T_2 \in \mathcal{T}_n$  for which  $T_1$  is adjacent to  $T_2$  but  $T_1 \cup T_2$  is not simply connected. When constructing  $F_n$ , I treat such adjacencies as illegal, and add clauses of the form  $s_{T_1,n} \rightarrow \neg s_{T_2,n}$  to prevent them.

However, it is also possible for the  $n$ -corona to contain a hole enclosed by three or more different copies of  $S$  (Figure 4, right). It would be prohibitive to precompute and suppress all possible holes formed by subsets of  $\mathcal{T}_n$ . Fortunately, such holes are exceedingly rare and can be eliminated one at a time as they arise, using a standard trick from discrete optimization. If I am trying to compute a shape’s hole-free Heesch number, and  $F_n$  is reported as satisfiable, I “draw” the implied packing by assigning symbolic colours to

Clause and quantifiers	Explanation
$s_{I,0}$	The 0-corona is always used.
$s_{T,k} \rightarrow c_p$ For all $0 \leq k \leq n$ For all $T \in \mathcal{T}_k$ For all $p \in T(S)$	If a copy of $S$ is used, then its cells are used.
$c_p \rightarrow s_{T_1,k_1} \vee \dots \vee s_{T_m,k_m}$ For all $0 \leq k_i \leq n$ For all $T_i \in \mathcal{T}_{k_i}$ Where $p \in T_i(S)$	If a cell is used, then some copy of $S$ must use it.
$s_{T,k} \rightarrow c_q$ For all $0 \leq k \leq n - 1$ For all $T \in \mathcal{T}_k$ For all $q \in \text{HALO}(T(S))$	If a copy of $S$ is used in an interior corona (a $k$ -corona for $k < n$ ), then that copy's halo cells must be used.
$s_{T_1,k_1} \rightarrow \neg s_{T_2,k_2}$ For all $0 \leq k_1, k_2 \leq n$ For all $T_1 \in \mathcal{T}_{k_1}$ and $T_2 \in \mathcal{T}_{k_2}$ Where $(T_1, k_1) \neq (T_2, k_2)$ And $T_1(S) \cap T_2(S) \neq \emptyset$	Used copies of $S$ cannot overlap.
$s_{T,k} \rightarrow s_{T_1,k-1} \vee \dots \vee s_{T_m,k-1}$ For all $1 \leq k \leq n$ For all $T_i \in \mathcal{T}_{k-1}$ Where $T_i$ is adjacent to $T$	If a copy of $S$ is used in a $k$ -corona, it must be adjacent to a copy in a $(k-1)$ -corona.
$s_{T_1,k} \rightarrow \neg s_{T_2,m}$ For all $2 \leq k \leq n$ Where $T_1 \in \mathcal{T}_k$ For all $0 \leq m \leq k-2$ For all $T_2 \in \mathcal{T}_m$ Where $T_2$ is adjacent to $T_1$	If a copy of $S$ is used in a $k$ -corona, it cannot be adjacent to a copy in an $m$ -corona for $m < k-1$ .

FIGURE 3. The clauses that make up the Boolean formula  $F_n$ , which is satisfiable if a shape  $S$  has an  $n$ -corona.

the grid cells in a 2D image, with colours that index the transformed copies of  $S$ . A simple algorithm such as flood filling can then search the packing for holes. If none are found, then  $S$  has  $H_c \geq n$  and the algorithm proceeds to testing  $F_{n+1}$ . If a hole is found, its boundary will be made up of cells belonging to shapes transformed by some set  $\{T_1, \dots, T_m\} \subset \mathcal{T}_n$ . I add a clause  $\neg s_{T_1,n} \vee \dots \vee \neg s_{T_m,n}$ , designed to prevent this precise hole, and re-run

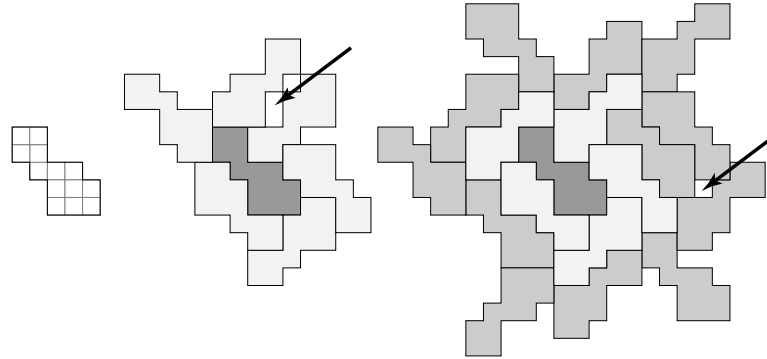


FIGURE 4. A nontiling 13-omino (left) that demonstrates the problem of detecting holes in the outermost corona. The middle illustration shows a 1-corona where two adjacent shapes enclose holes (one is indicated by an arrow). These holes can be suppressed by including a clause forbidding the two shapes from both being used. On the right, the 2-corona includes a hole bounded by three copies of the shape. Such holes are difficult to prevent and are explicitly forbidden after the fact if they are found.

the SAT solver. By repeating his process, eventually we will either find a hole-free solution, or the solver will report the enriched  $F_n$  as unsatisfiable, implying that  $S$  has  $H_c < n$ . Unfortunately, verifying that a patch is simply connected is necessary and potentially expensive; after initial preprocessing, it is the only part of the process that relies on the actual geometry of the problem rather than its reduction to Boolean logic. I am not aware of an effective way to design  $F_n$  to force the  $n$ -corona to be simply connected at the outset.

As mentioned in section 2.1, it is theoretically possible for a hole to arise in a  $k$ -corona, which can then be perfectly filled by additional shapes. This possibility cannot be explicitly forbidden by the Boolean formulas developed in this work, and would not be detected by the hole suppression techniques (it would be necessary to check that every corona is connected, in addition to their union). If we can surround the outer boundary of this  $k$ -corona, we could think of the union of the surround and the hole fillers as a  $(k+1)$ -corona split into two disconnected pieces. That expanded view would open the door to highly disorderly coronas, though the circumstances that produce them must be vanishingly rare. In practice, I ignore this possibility and assume that holes are unfillable.

#### 4. GENERAL POLYFORMS

The geometry of polyominoes makes them easy to work with computationally and simplifies the development of the previous section. All the

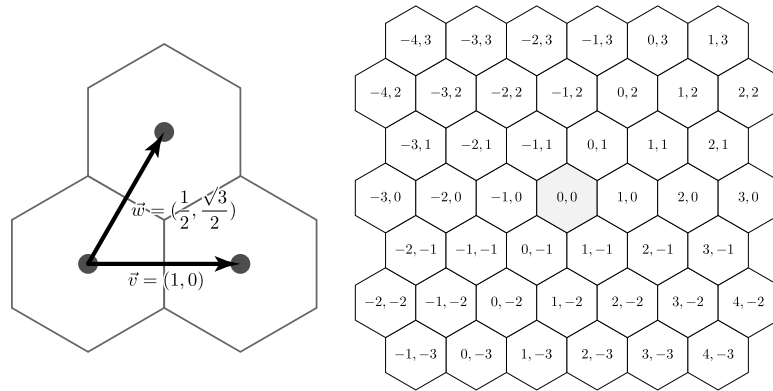


FIGURE 5. The basis on the left allows every cell in an infinite hexagonal tiling to be assigned a unique pair of integer coordinates.

geometric computations above can be represented quite compactly in software. If we assume that we will not enumerate beyond 23-ominoes (already an ambitious goal!), and that Heesch numbers will not exceed 5, then any conceivable set of coronas will fit inside a  $256 \times 256$  grid, meaning that a cell coordinate can fit in a single signed byte. By the same token, a transformation can easily fit in 32 bits: at a minimum, we require eight bits each for the coordinates of the translation, and three more to select a combination of rotation and reflection. Furthermore, any copy of a shape  $S$  can be represented implicitly via its transformation, meaning that construction of  $F_n$  can be carried out entirely with 32-bit integers, regardless of the size of  $S$ . It is only when checking whether a patch is simply connected that I resort to instantiating a large grid and drawing copies of  $S$  in it.

The SAT reduction above can be adapted to other classes of polyforms, provided that they are expressible as subsets of a fixed ambient tiling. That easily encompasses the regular tilings by hexagons and equilateral triangles, giving us polyhexes and polyiamonds. It rules out, for example, shapes formed from edge-to-edge assemblies of isosceles right triangles, sometimes known as *polyabolos* or *polytans*. Of course, even with polyhexes and polyiamonds, we would like to keep the representation of shapes and transformations simple, compact, and discrete. The solution is to express all coordinates relative to nonstandard basis vectors. This trick is fairly common when working with hexagonal grids in software, but I will summarize the approach here.

**4.1. Polyhexes.** The cells in a hexagonal grid can be assigned integer coordinates in a basis with vectors  $\vec{v} = (1, 0)$  and  $\vec{w} = (1/2, \sqrt{3}/2)$ , connecting a hexagon centre to the centres of two of its neighbours. The basis is illustrated in Figure 5, together with a portion of a grid labelled with coordinate pairs.

A hexomino has a maximum of 12 distinct orientations, six direct and six reflected. They are generated by a transformation  $A$  that rotates by  $60^\circ$  about the origin, and a transformation  $B$  that reflects across the  $\vec{v}$  axis. Working in the basis  $\{\vec{v}, \vec{w}\}$ , these transformations have simple representations as matrices with integer entries:

$$A = \begin{bmatrix} 0 & -1 \\ 1 & 1 \end{bmatrix}, \quad B = \begin{bmatrix} 1 & 1 \\ 0 & -1 \end{bmatrix}.$$

The products  $A^i B^j$  for  $i = 0, \dots, 5$  and  $j = 0, 1$  yield matrices for all 12 orientations which, like their square counterparts, all have entries in  $\{-1, 0, 1\}$ . These can be combined with translations by vectors with integer coordinates to represent all possible transformations of a polyhex.

To construct the halo of a polyhex  $S$ , we must consider every cell in the *6-neighbourhood* (and not the 8-neighbourhood) of a given cell. These six neighbours can easily be found by offsetting the coordinates of a cell by the six coordinate pairs in the ring around  $(0, 0)$  in Figure 5. The revised definition of  $\text{HALO}(S)$  also affects the definition of adjacency and by extension a number of the clauses that make up  $F_n$ .

When suppressing holes, verifying that a packing of polyhexes is simply connected also depends on the distinct topology of the hexagonal grid. It is still possible to draw the packing directly into a square image using the cells' integer coordinates and to use a flood fill to detect holes. But unlike the square case, after filling an empty grid cell the algorithm must walk recursively to the empty cells in its 6-neighbourhood.

**4.2. Polyiamonds.** Polyiamonds are slightly more complicated than polyominoes or polyhexes, in that there are two possible orientations for cells in the infinite tiling by equilateral triangles. So, for example, translations cannot simply bring any triangle into correspondence with any other—they must respect orientation. I build a somewhat exotic sparse integer representation of the triangular grid that harnesses the hexagonal representation described above.

Figure 6 shows part of a triangular grid on the left, with upward-pointing black triangles and downward-pointing grey triangles. The illustration on the right shows how triangles are assigned coordinates in the hexagonal grid. Every black triangle has coordinates that are divisible by 3; every grey triangle has coordinates that are congruent to 1 modulo 3. Other hexagonal cells are simply left unused.

Like a polyhex, a polyiamond has a maximum of twelve orientations. Six of these correspond to automorphisms of the black triangle at  $(0, 0)$  in Figure 6, and can be found among the orientation matrices for hexominoes. The other six combine one of these six transformations with a transformation that swaps black and grey triangles, for example, an application of  $B$  above followed by a translation by  $(1, -2)$ . Any transformation of a polyiamond

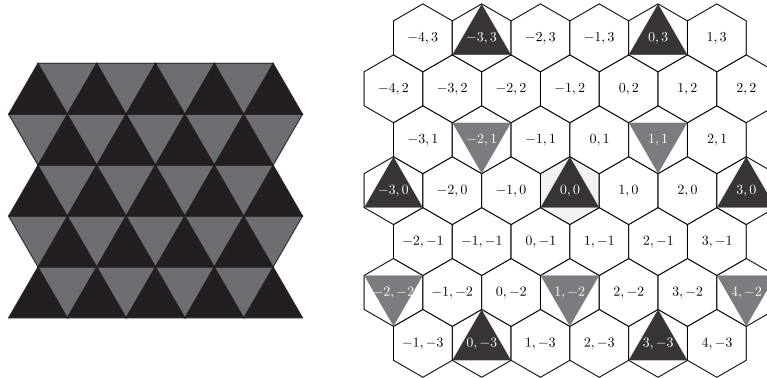


FIGURE 6. Polyiamonds can be represented efficiently using a sparse subset of the hexagonal grid. The conceptual tiling on the left is spread out to the shaded cells in the hexagonal tiling on the right.

can be represented by a choice of orientation together with a translation by a vector whose coordinates are divisible by 3.

Neighbourhoods must also be reconsidered in this model. When computing haloes we must take into account the 12-neighbourhood of each cell in a polyiamond  $S$ , consisting of all cells that share an edge or a vertex with the given cell. In Figure 6, the 12-neighbourhood of  $(0, 0)$  consists of every other black and grey triangle shown, together with one more at  $(-2, 4)$ . The 12-neighbourhood is fine when computing haloes and determining adjacency, but not when checking a packing for holes. In that case, a flood fill algorithm should move from a given cell only to the three neighbours with which it shares an edge.

## 5. IMPLEMENTATION AND RESULTS

I have implemented the data structures and algorithms described here as a C++ program. The geometry and topology of the underlying grid (square, hexagonal, or triangular) is abstracted into a `Grid` class that can be used as a template parameter when launching the algorithm. The core computation of Heesch numbers can then be written once relative to a wide range of possible polyform types. The program reads a sequence of polyforms in plain text format and produces a text report with the values of  $H_c$  and  $H_h$  for the input shapes. A command line option causes the program to include, for each shape, the set of transformations that make up the coronas in the packings found by the SAT solver. A separate Python script can read the shape description and transformations and draw the coronas that realize the shape's computed Heesch number.

The program is unable to determine whether a shape tiles the plane, and must be given known nontilers as input. I use software written by Joseph

$n$	nontilers	$H_c = 0$	$H_c = 1$	$H_c = 2$	$H_c = 3$
7	3	1	2		
8	20	6	14		
9	198	75	122	1	
10	1390	747	642	1	
11	9474	5807	3628	39	
12	35488	28572	6906	10	
13	178448	149687	28694	67	
14	696371	635951	60362	58	
15	2721544	2598257	123262	25	
16	10683110	10397466	285578	66	
17	41334494	40695200	639162	130	2
18	155723774	154744331	979375	68	
19	596182769	593856697	2325874	198	

TABLE 1. Heesch numbers of  $n$ -ominoes with no holes in the outer corona.

Myers [11] to enumerate free polyforms (which are unique up to rotation and reflection) and discard the shapes that tile. I then use a separate program to convert from the representation Myers uses in his output (a boundary word made up of unit steps from an alphabet of evenly spaced directions) to an area-based representation (coordinates of cells that make up a polyform).

I use the open-source CryptoMiniSat library [12] as my SAT solver. The library is easy to configure, has a simple C++ API, and performs well in practice. It may be worthwhile to investigate the merits of other SAT solvers, such as Glucose [1], which may contain heuristics that are better tuned to the Boolean formulas used in Heesch number computation.

In this work, we are evaluating billions of SAT instances, each of which is relatively modest in size by modern standards. Therefore, while different SAT libraries support varying amounts of parallelization, it is far more expedient in this case simply to distribute the individual shapes over multiple CPU cores and allow the SAT solver to use a single thread on each one. I divide nontiling polyforms into batches of thousands or tens of thousands, and hand off batches to processes running on different cores.

A SAT solver imposes a small amount of overhead on running time, because of the need to translate problems from their geometric origins into Boolean formulas. However, the benefits of the solver more than compensate for this added cost. Human intuition is easily seduced by the structure of a geometric problem, and that intuition colours the choice of the algorithm used in solving the problem. Sometimes the resulting algorithms are perfectly fine. But here, a “natural” approach—walking around the boundary of a shape, gluing on neighbours, and backtracking when no legal option exists for continuing—can get stuck in “backtracking hell”. An unavoidable dead end may lurk far out along the boundary of a shape, with exponentially

$n$	nontilers	$H_h = 0$	$H_h = 1$	$H_h = 2$	$H_h = 3$
7	3	0	3		
8	20	0	19	1	
9	198	36	157	5	
10	1390	355	1020	15	
11	9474	2820	6544	109	1
12	35488	17409	18038	41	
13	178448	100180	78048	219	1
14	696371	485807	210362	202	
15	2721544	2185656	535724	164	
16	10683110	9300840	1381965	305	
17	41334494	37932265	3401701	525	3
18	155723774	148955184	6768266	324	
19	596182769	580412188	15769814	767	

TABLE 2. Heesch numbers of  $n$ -ominoes with holes permitted in the outer corona.

$n$	nontilers	$H_c = 0$	$H_c = 1$	$H_c = 2$	$H_c = 3$	$H_c = 4$
6	4		3	1		
7	37	5	25	6	1	
8	381	70	264	44	3	
9	2717	825	1822	67	3	
10	18760	8248	10234	265	13	
11	116439	67644	47940	817	37	1
12	565943	431882	133484	567	10	
13	3033697	2565727	466159	1783	27	1
14	14835067	13676416	1156793	1836	22	
15	72633658	69871458	2758485	3534	179	2
16	356923880	350337478	6581529	4818	54	1
17	1746833634	1731652467	15167876	13129	161	1

TABLE 3. Heesch numbers of  $n$ -hexes with no holes in the outer corona.

many (or more!) configurations of neighbours to be explored along the way, all of which will be rejected. The earlier work of Mann and Thomas [10] attempts to surround in a fixed order, and they report a number of cases where their algorithm times out. A SAT solver has no particular opinion on the geometric structure of the problem domain. Its input is an undifferentiated collection of clauses, and it will take advantage of any opportunity it can find to narrow the search space, regardless of order or locality.

I have not attempted to gather full information about the running times of these programs. On a single core of a 40-CPU cluster node with 2.2 GHz Intel Xeon processors, I can compute the Heesch numbers of all 1390

$n$	nontilers	$H_h = 0$	$H_h = 1$	$H_h = 2$	$H_h = 3$	$H_h = 4$
6	4		3	1		
7	37	4	19	12	2	
8	381	37	253	84	7	
9	2717	434	2091	185	7	
10	18760	4332	13766	632	29	1
11	116439	38621	75783	1956	73	6
12	565943	286656	277601	1652	32	2
13	3033697	1895666	1132994	4985	50	2
14	14835067	11201813	3627594	5614	46	
15	72633658	61761205	10862327	9802	322	2
16	356923880	325357916	31551809	13997	156	2
17	1746833634	1660634503	86167750	30811	569	1

TABLE 4. Heesch numbers of  $n$ -hexes with holes permitted in the outer corona.

$n$	nontilers	$H_c = 0$	$H_c = 1$	$H_c = 2$	$H_c = 3$	$H_c = 4$
7	1		1			
8	0					
9	20	11	9			
10	103	44	55	3	1	
11	594	236	346	11	1	
12	1192	826	364	1	1	
13	6290	4360	1884	24	2	
14	18099	14949	3141	8		
15	54808	48108	6661	39		
16	159048	148881	10153	13	1	
17	502366	474738	27544	83	1	
18	1374593	1341460	33100	33		
19	4076218	4001470	74689	57	2	
20	11378831	11282686	96091	51	2	1
21	32674779	32505745	168959	73	2	
22	93006494	92740453	265977	62	2	
23	264720498	264216706	503651	140	1	
24	748062099	747476118	585571	384	26	

TABLE 5. Heesch numbers of  $n$ -iamonds with no holes in the outer corona.

nontiling 10-ominoes in about 220 seconds, on average about 0.16 seconds per shape. I have also sampled the running times on batches of the much larger 17-hexes, and the average per-shape computation time is comparable. Unsurprisingly, the computation time appears to increase exponentially for shapes with higher Heesch numbers. For example, shapes with Heesch

$n$	nontilers	$H_h = 0$	$H_h = 1$	$H_h = 2$	$H_h = 3$	$H_h = 4$
7	1		1			
8	0					
9	20	7	13			
10	103	33	59	10		1
11	594	117	446	30	1	
12	1192	495	692	4	1	
13	6290	2639	3598	51	2	
14	18099	10328	7745	25		
15	54808	36965	17748	91	4	
16	159048	124954	34058	35	1	
17	502366	414119	88072	173	2	
18	1374593	1239971	134541	80	1	
19	4076218	3776105	299954	157	2	
20	11378831	10921532	457157	139	2	1
21	32674779	31831654	842947	174	4	
22	93006494	91551851	1454494	147	2	
23	264720498	262051399	2668753	343	3	
24	748062099	744472222	3589353	425	99	

TABLE 6. Heesch numbers of  $n$ -iamonds with holes permitted in the outer corona.

number 4 might require 30 seconds to a minute of computation time. But because such shapes become progressively more rare as the Heesch number increases, the overall effect on computation time is negligible.

Tables 1–6 list Heesch numbers for all the nontiling polyforms I tested, up to 19-ominoes, 17-hexes, and 24-iamonds. For values of  $n$  smaller than those shown in the tables, no nontilers exist. Permitting holes in the outermost corona offers shapes more freedom to form coronas. As a result, the rows of the  $H_h$  tables are weighted slightly more to the right than the corresponding rows of the  $H_c$  tables.

Of course, a few highlights deserve to be shared. I am particularly interested in the smallest polyforms that exhibit each successive Heesch number. Figure 1 already shows the smallest polyominoes with  $H_c = 1$  and  $H_h = 1$ . Figure 7 shows the smallest polyominoes with Heesch numbers 2 and 3, both with and without holes. In Figures 8 and 9, I show the smallest polyhexes and polyiamonds with hole-free Heesch numbers 1 through 4. In all cases, my search did not produce any shapes with Heesch numbers higher than the ones shown.

A larger dataset, containing text descriptions and drawings of shapes with high Heesch numbers, can be found at [www.cs.uwaterloo.ca/~csk/heesch/](http://www.cs.uwaterloo.ca/~csk/heesch/).

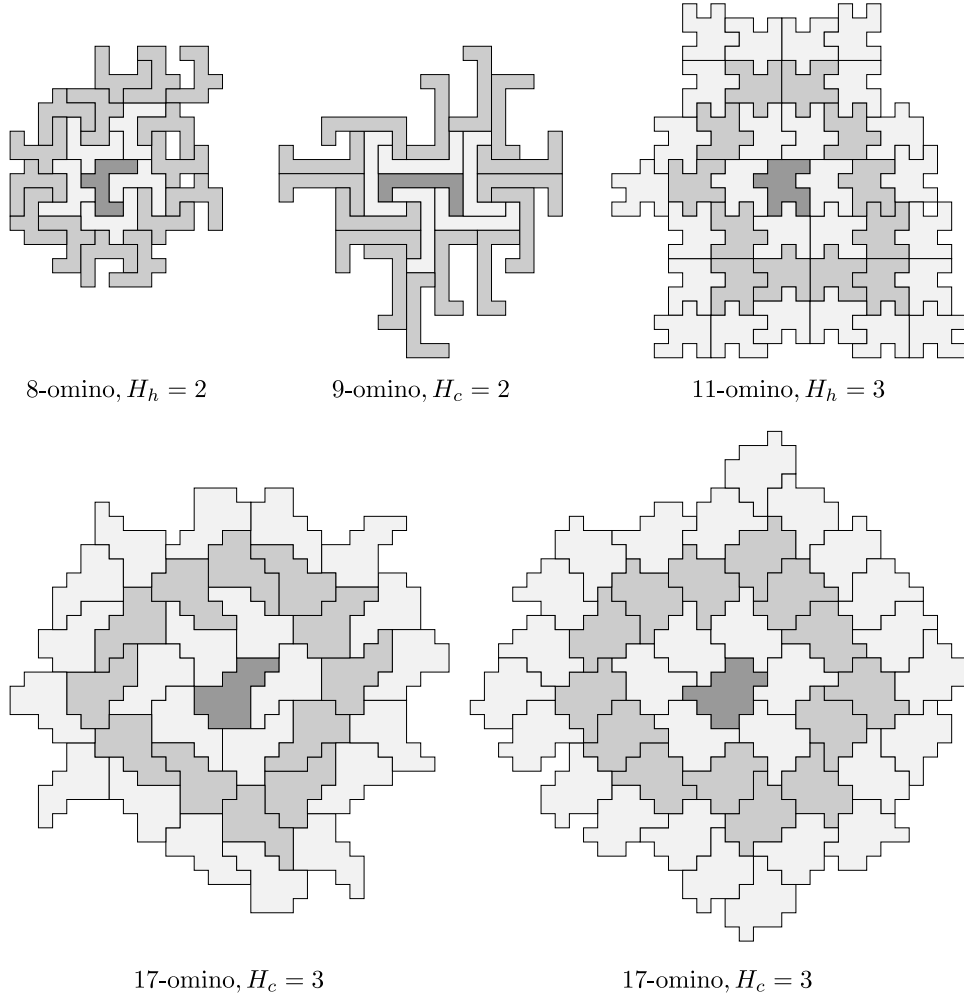


FIGURE 7. The smallest polyominoes with Heesch numbers 2 and 3, with and without holes in the outermost corona. The 11-omino has a single square hole on the right side of the packing.

## 6. CONCLUSIONS

In this article, I have demonstrated the effectiveness of recasting the computation of Heesch numbers within the framework of Boolean satisfiability. I used a software implementation of this idea to compute Heesch numbers for a few billion unmarked polyominoes, polyhexes, and polyiamonds. The search did not yield any shapes that break previous records for Heesch numbers but provides a lot of data that can be used to deepen our understanding of this intriguing open problem in tiling theory.

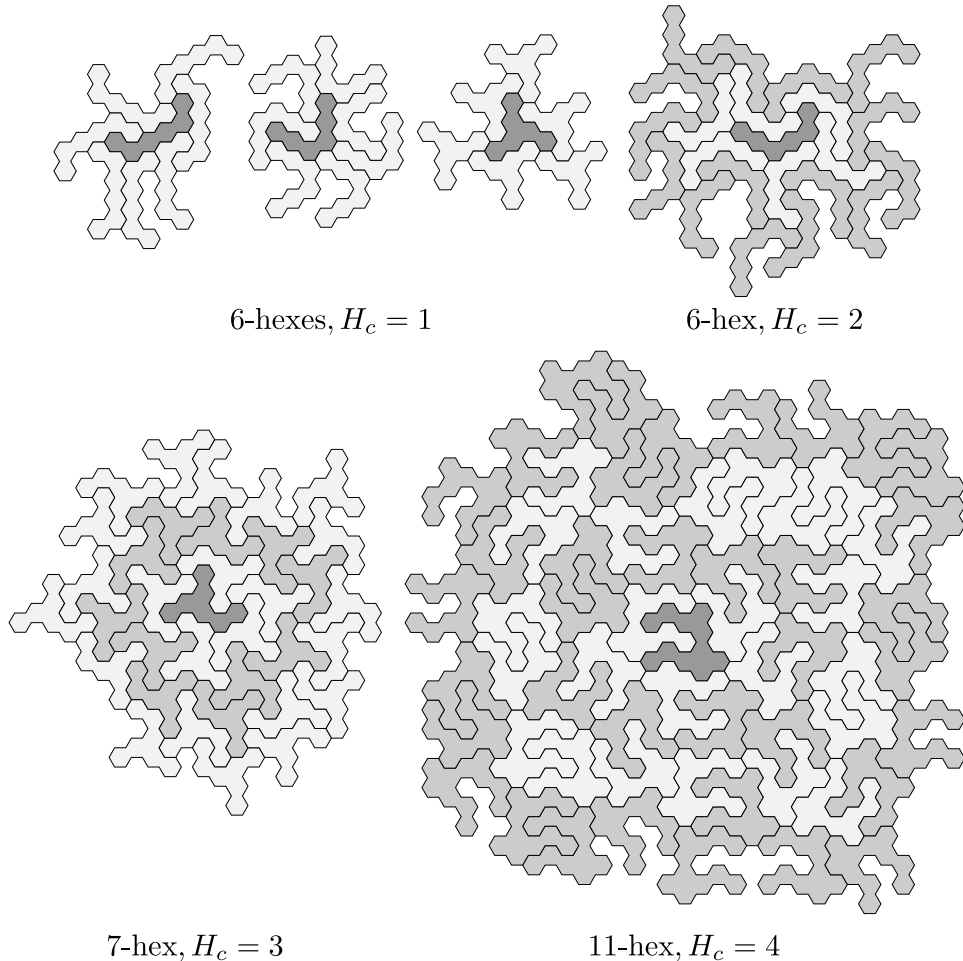


FIGURE 8. The smallest polyhexes with  $H_c = 1, 2, 3, 4$ .

The most obvious avenue for future work is to continue the enumeration to larger polyforms. However, I am reluctant to do so without significant performance improvements or insights on narrowing the set of polyforms to process. For example, there are more than twice as many nontiling 18-hexes as all the Heesch numbers I have computed so far: over 8.5 billion of them. If they require an average of 0.15 seconds each to process, I estimate that a 120-core cluster would have to run full-tilt for four months to compute them all.

It would be interesting to reformulate the approach presented here using binary integer programming [7] instead of Boolean satisfiability. Some families of clauses might be expressed much more compactly this way. With satisfiability, if transformed shapes  $T_1(S), \dots, T_m(S)$  all overlap at some cell,

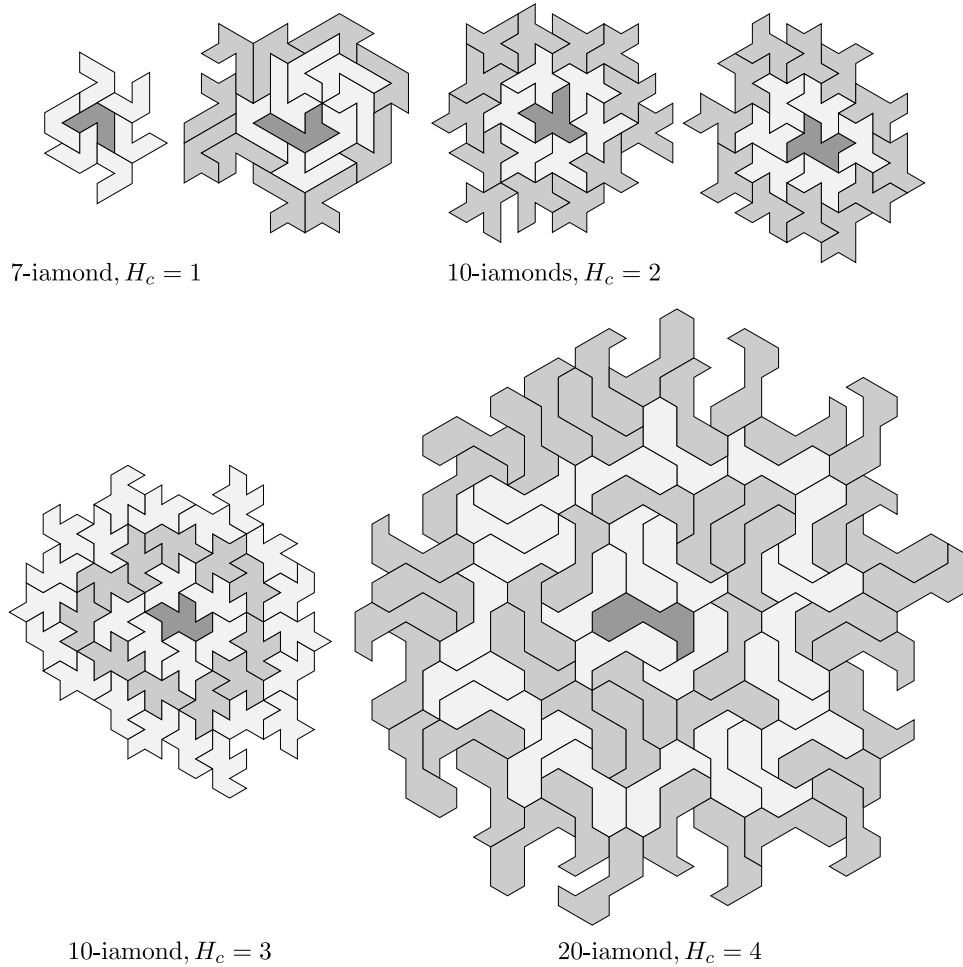


FIGURE 9. The smallest polyiamonds with  $H_c = 1, 2, 3, 4$ .

then  $\binom{m}{2}$  clauses of the form  $s_{T_i, k_i} \rightarrow \neg s_{T_j, k_j}$  are required to rule out all possible overlaps. In binary integer programming, the shape variables would be assigned the integers 0 or 1, and all overlaps at this cell could be prevented with the single inequality  $s_{T_1, k_1} + \dots + s_{T_m, k_m} \leq 1$ . (Some SAT solvers allow XOR-style clauses that might be able to achieve a similar effect.) However, it is unclear whether this change would boost performance.

Part of the goal of assembling a large corpus of data is to mine it for patterns. I do not believe that the tables in this article betray any obvious patterns in the sizes of polyforms that produce certain Heesch numbers. The general upward trend in each column could be a simple consequence of the exponential growth in the number of shapes being classified, and even then the numbers jump around erratically. But there may be some insight to be gleaned from examinations of the shapes themselves. Mann and Thomas

refer to “forced grouping”, in which tiles in a patch tend to cluster together into larger units [10]. I have observed this phenomenon in many of my results as well—see for example the 11-hex patch in Figure 8. Forced grouping may inspire strategies for “amplifying” the Heesch number of a large shape by finding a way to decompose it into smaller congruent pieces.

Perhaps the most promising way forward is to consider other families of shapes. The techniques in this article could easily be extended to handle marked polyforms, simply by prohibiting adjacencies that are not compatible with the markings. However, it would be crucial to apply markings to polyforms that tile the plane. Markings can only lower an unmarked shape’s Heesch number, making it pointless to add markings to any of the polyforms presented here. It would therefore become necessary to check explicitly that a set of markings prevents a polyform from tiling, whether based on combinatorial imbalance or a more complex computation. Of course, it would be interesting to explore the use of a SAT solver (or integer programming) to check whether a shape tiles the plane.

It may also be possible to extend this work to polyforms built from other ambient grids, such as unions of squares and octagons, or triangles and hexagons. We might also consider more flexible polyforms that do not use a fixed grid, like the polyabolos mentioned previously, or shapes constructed from unions of Penrose rhombs. In that case, we would likely have to do away with haloes and cell variables, and use techniques from computational geometry to test whether two copies of a shape are disconnected, adjacent, or overlapping. The lack of a grid to organize the plane would incur a heavy cost, but the greater potential for disorder may pack higher Heesch numbers into smaller shapes.

#### ACKNOWLEDGMENTS

I am deeply grateful to Bram Cohen, who first proposed using a SAT solver to compute Heesch numbers, suggested a lot of the Boolean logic, and acted as a sounding board throughout the work. Many thanks also to Joseph Myers, who shared his code for checking the tiling properties of polyforms and helped me use it to good effect. Erik Demaine, Alex Kontorovich, and Casey Mann all provided valuable feedback during the preparation of this manuscript, helping to steer it towards publication in a research area outside my normal expertise. Thanks to Lori Paniak for assistance running some processes on an in-house compute cluster. This work was made possible by the facilities of the Shared Hierarchical Academic Research Computing Network (SHARCNET) and Compute/Calcul Canada.

#### REFERENCES

1. G. Audemard and L. Simon, *Predicting learnt clauses quality in modern SAT solvers*, Twenty-first International Joint Conference on Artificial Intelligence, 2009.
2. B. Bašić, *A figure with Heesch number 6: Pushing a two-decade-old boundary*, The Mathematical Intelligencer (2021), 1–4.

3. R. Berger, *The undecidability of the domino problem*, Memoirs of the American Mathematical Society, no. 66, American Mathematical Soc., 1966.
4. A. Fontaine, *An infinite number of plane figures with Heesch number two*, Journal of Combinatorial Theory, Series A **57** (1991), no. 1, 151–156.
5. C. Goodman-Strauss, *Open questions in tiling*, <https://strauss.hosted.uark.edu/papers/survey.pdf>, 2000, Accessed: May 14th, 2021.
6. B. Grünbaum and G. C. Shephard, *Tilings and patterns*, second ed., Dover, 2016.
7. LLC Gurobi Optimization, *Gurobi optimizer reference manual*, 2021.
8. C. S. Kaplan, *Introductory tiling theory for computer graphics*, Morgan & Claypool, 2009.
9. C. Mann, *Heesch's tiling problem*, The American Mathematical Monthly **111** (2004), no. 6, 509–517.
10. C. Mann and B. C. Thomas, *Heesch numbers of edge-marked polyforms*, Experimental Mathematics **25** (2016), no. 3, 281–294.
11. J. Myers, *Polyomino, polyhex and polyiamond tiling*, <https://www.polyomino.org.uk/mathematics/polyform-tiling/>, 2019, Accessed: May 14th, 2021.
12. M. Soos, K. Nohl, and C. Castelluccia, *Extending SAT solvers to cryptographic problems*, Theory and Applications of Satisfiability Testing - SAT 2009, 12th International Conference, SAT 2009, Swansea, UK, June 30 - July 3, 2009. Proceedings (Oliver Kullmann, ed.), Lecture Notes in Computer Science, vol. 5584, Springer, 2009, pp. 244–257.

SCHOOL OF COMPUTER SCIENCE, UNIVERSITY OF WATERLOO  
E-mail address: csk@uwaterloo.ca